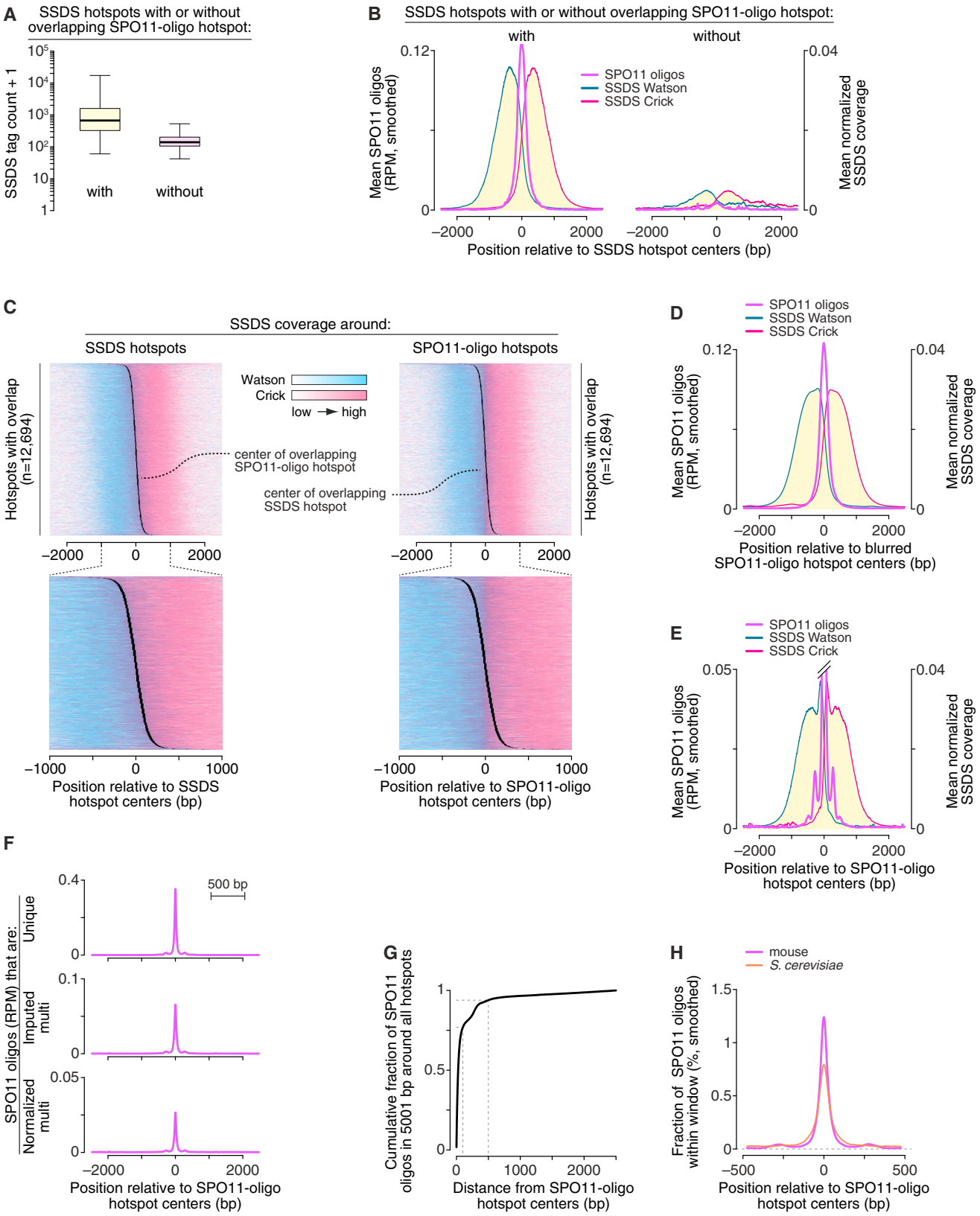

(legend on next page)

Figure S2. Features of SPO11-Oligo Hotspots, Related to Figure 2

(A) SSDS hotspots with an overlapping SPO11-oligo hotspot are substantially stronger than those without an overlapping SPO11-oligo hotspot. In the box plots, thick horizontal lines indicate medians, box edges show the 25th and 75th percentiles, and whiskers indicate lowest and highest values within 1.5-fold of the interquartile range; outliers are not shown.

(B) Distribution of SPO11 oligos (smoothed with a 51-bp Hann filter) and SSDS coverage around centers of SSDS hotspots with or without an overlapping SPO11-oligo hotspot. Note that a small peak of SPO11 oligos was present even for the non-overlapping set of SSDS hotspots.

(C) Hotspot centers are defined more precisely by SPO11-oligo mapping. Panels show heat maps of Watson and Crick SSDS coverage around hotspot centers as defined by SSDS (left panels) or by SPO11-oligo mapping (right panels). The normalized SSDS coverage across each 5010-bp window was binned in 10-bp bins. Because locally normalized coverage was used, color-coding reflects spatial patterns within hotspots and not relative intensity between hotspots. Only the 12,694 hotspots called in both datasets are shown and are ordered in each plot by center-to-center distance between the alternative center definitions. The black line in each plot indicates the center position of the matched hotspot as defined in the alternative dataset. The SPO11-oligo hotspot centers track more faithfully with the switch between Watson and Crick SSDS coverage: compare the black lines to the boundary between red and blue SSDS signal (left and right panels), and note that this boundary lines up vertically across all hotspots when aligned by the SPO11-oligo hotspot center definition (right panels).

(D) Reducing the precision of SPO11-oligo hotspot definitions recapitulates genome averages derived from SSDS hotspot center definitions. Resection uncovers tracts of ssDNA that are much longer than the width of most DSB hotspots, and sequencing of DMC1-bound ssDNA by SSDS displays marked local biases. (Note the strong peaks-and-valleys appearance of the SSDS maps around *A3* as an example; Figure 1E). These two features would be predicted to negatively affect the precision in estimating DSB hotspot centers. In contrast, the 5′ ends of SPO11 oligos are more directly and precisely tied to DSB positions per se, and SPO11 oligos derive from narrow zones. Thus, centers of SPO11-oligo hotspots are predicted to provide a more precise estimate of true DSB hotspot centers. To test this conclusion, we artificially blurred the precision of SPO11-oligo hotspot centers and examined resulting average patterns in the SPO11-oligo and SSDS datasets. We first determined, for overlapping SPO11-oligo and SSDS hotspots, the distribution of distances between the hotspot centers defined by the two methods (range: −1676 to +1634 bp). We then sampled with replacement from that distribution to shift the location of each SPO11-oligo hotspot center in the 5′ or 3′ direction. The simulation was run 1000 times. As expected, when we plotted SPO11 oligos (smoothed with a 51-bp Hann filter) and SSDS coverage around these blurred centers, we reconstituted the average patterns observed around SSDS hotspot centers (compare with Figure 1G). We conclude that the SPO11-oligo map more accurately reflects the fine-scale distribution of recombination initiation in mice.

(E) Distribution of SPO11 oligos (51-bp Hann filter) and SSDS coverage around SPO11-oligo hotspot centers. Data are the same as in Figure 2D, but zoomed into the lower range of SPO11-oligo values to focus on secondary peaks.

(F) The average patterns of unique reads, imputed multi-mapped reads, and normalized multi-mapped reads around the centers of SPO11-oligo hotspots are similar. Each map was plotted as RPM of the total 69.4 million reads mapped to the nuclear genome and was smoothed with a 51-bp Hann filter.

(G) Cumulative fraction, by distance from hotspot centers, of SPO11 oligos around all hotspots. Of the 29.4 million SPO11-oligo reads that mapped within 2500 bp of hotspot centers, 76.9% were within 100 bp of hotspot centers and 93.9% within 500 bp.

(H) Comparison of average SPO11-oligo profiles around mouse and *S. cerevisiae* hotspots. The profile from each species is scaled to yield matched areas under the curves for the regions shown. Note that the average for budding yeast hotspots is less compact than the central peak for mouse, as indicated by the lower height and greater width for yeast. In both species, hotspot substructure appears to be strongly shaped by the underlying chromatin structure. This substructure shows more variation between hotspots in budding yeast because the NDRs in gene promoters that are targeted by Spo11 show more variation from one to another.